THE JOURNAL OF PHYSICAL CHEMISTRY B

Article

pubs.acs.org/JPCB

Modeling Copper Binding to the Amyloid-β Peptide at Different pH: Toward a Molecular Mechanism for Cu Reduction

Sara Furlan,[†] Christelle Hureau,[†] Peter Faller,[†] and Giovanni La Penna*[,‡]

[†]LCC - Laboratory of coordination chemistry, CNRS - National Center for Scientific Research, 205 route de Narbonne, F-31077 Toulouse, France

[‡]ICCOM - Institute for chemistry of organo−metallic compounds, CNR - National Research Council of Italy, via Madonna del Piano 10, I-50019 Sesto Fiorentino, Firenze, Italy

Supporting Information

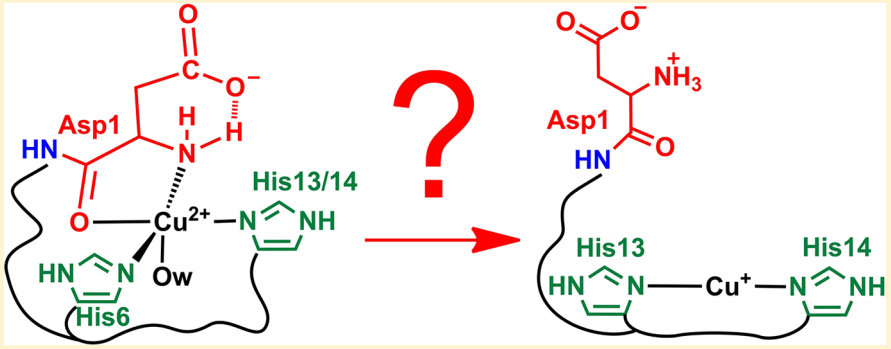

ABSTRACT: Oxidative stress, including the production of reactive oxygen species (ROS), has been reported to be a key event in the etiology of Alzheimer's disease (AD). Cu has been found in high concentrations in amyloid plaques, a hallmark of AD, where it is bound to the main constituent amyloid-β (Aβ) peptide. Whereas it has been proposed that Cu-Aβ complexes catalyze the production of ROS via redox-cycling between the Cu(I) and Cu(II) state, the redox chemistry of Cu-Aβ and the precise mechanism of redox reactions are still unclear. Because experiments indicate different coordination environments for Cu(II) and Cu(I), it is expected that the electron is not transferred between Cu-Aβ and reactants in a straightforward manner but involves structural rearrangement. In this work the structures indicated by experimental data are modeled at the level of modern density-functional theory approximations. Possible pathways for Cu(II) reduction in different coordination sites are investigated by means of first-principles molecular dynamics simulations in the water solvent and at room temperature. The models of the ligand reorganization around Cu allow the proposal of a preferential mechanism for Cu-Aβ complex reduction at physiological pH. Models reveal that for efficient reduction the deprotonated amide N in the Ala 2-Glu 3 peptide bond has to be protonated and that interactions in the second coordination sphere make important contributions to the reductive pathway, in particular the interaction between COO^- and NH_2 groups of Asp 1. The proposed mechanism is an important step forward to a clear understanding of the redox chemistry of Cu-Aβ, a difficult task for spectroscopic approaches as the Cu-peptide interactions are weak and dynamical in nature.

INTRODUCTION

Copper ions play a key role in a multitude of biological processes, mostly in the active center of enzymes where a major function is in electron transfer reactions and/or substrate binding. Most prominent are superoxide dismutase and cytochrome c oxidase. In biology, copper can occur in two stable redox states, Cu(I) and Cu(II). The redox reactions are mostly restricted to these two redox states and hence include a one electron transfer per Cu ion. These ions are classically strongly bound in the enzymes, in both thermodynamic and kinetic sense. Loosely bound or free Cu ions can undergo uncontrolled redox reactions and are able to promote the reduction of dioxygen, and hence the production of reactive oxygen species (ROS), which are potentially harmful to cells due to their reaction with proteins, nucleic acids, and lipids. To avoid these last reactions, the Cu metabolism is tightly controlled with the help of Cu transmembrane transporters and Cu chaperones (intracellular carriers).[1−4]

Under stress or disease conditions, Cu homeostasis can be affected, leading to more loosely bound Cu, prone to ROS production.[5] This is thought to be the case in neurodegenerative disorders,[6] including Alzheimer's disease (AD),[7−9] where a high concentration of Cu is found in amyloid plaques, a hallmark of this disease. Cu is bound to the main constituent, the peptide amyloid-β (Aβ).[10] Thus, it is thought that Cu is bound to Aβ under AD conditions, and it

Received: September 10, 2012
Revised: September 13, 2012
Published: September 13, 2012

has been also shown that Cu-Aβ is redox competent and able to catalytically produce ROS in the presence of physiological concentrations of a reductant like ascorbate.[11]

The coordination chemistry of Cu(II) and Cu(I)-Aβ has been the subject of a multitude of studies.[12] The binding of either Cu ion to the Aβ peptide is very dynamic and different binding environments are in fast exchange.[13] For instance the main binding mode for Cu(I) is a digonal coordination to the Nδ of the two His 13 and His 14.[12,14,15] However, this main coordination is in fast exchange with the same digonal binding including His 6.[15,16] At physiological pH, Cu(II) is bound to Aβ in two different coordination sites. In the major form (usually noted I), Cu(II) is bound to four equatorial ligands: the terminal NH_2 of Asp 1, the adjacent C=O group of the Asp 1—Ala 2 peptide bond, and the side chains of His 6 and His 13 or His 14 (the latter in exchange). In the minor form (usually noted as II), the Cu(II) equatorial ligands are NH_2 (Asp 1), the deprotonated amide N of the Asp 1—Ala 2 bond, the adjacent C=O from the Ala 2—Glu 3 bond, and one of the His side chains[13,17] (Figure 1, top).

As the redox cycling between Cu(I)- and Cu(II)-Aβ is the underlying mechanism of ROS production, several studies have been reported in the literature,[18−20] showing the intricacy of electrochemical results. Very recently, Balland et al.[21] suggested a very original redox mechanism (preorganized electron transfer, POET) on the basis of extensive cyclic voltammetry studies. In line with the highly different structures of the main coordination modes observed for Cu(I) and Cu(II)-Aβ, the redox reaction is very sluggish. In fact, the redox process goes through a very low populated state (about 0.1%), in which electron transfer is very fast because the reorganization energy, in this particular state, is very low. This preorganized state is in equilibrium with the Cu(I)- and Cu(II)-Aβ resting state complexes. Considering the very low population of this state, in exchange with the other spectroscopically observed states, it will be extremely difficult to study its structure by experimental techniques. Therefore, we used a modeling approach to gain a deeper insight into the reduction pathway of Cu(II) in the two coordination sites (I and II). We show here that the conformation and protonation state of the amide Asp 1—Ala 2 peptide bond can be the gate keeper for Cu(II) reduction and we report on potential candidates for the low populated redox competent state.

METHODS

For each of the models investigated in this work, four stages are performed, similarly to the modeling procedure applied to Cu(I)-Aβ(1−16).[16]

1. An empirical model for the complex, including the Cu ion, is used to search for nonoverlapping structures of Cu-Aβ(1−16) satisfying the conditions imposed by experiments in terms of coordination geometry. Monte Carlo random walks (MC-RW) are used in some cases.
2. Selected configurations are truncated to a first-principles manageable model and are merged into a simulation cell filled with water molecules and eventually counterions to neutralize the simulation cell.
3. An empirical model for the cell is simulated to provide a configuration for solvent molecules and counterions consistent with in vitro room conditions (water solution of the complex).
4. The final configuration of the previous step is then simulated within a density-functional (DFT) model and using the extended lagrangian formalism (Car−Parrinello molecular dynamics, CP-MD).

The details of the procedure are reported in the Supporting Information. The models, after a further simplification, are also studied in the vacuum for analyzing electronic structures and for comparisons with solvated models.

Despite the inclusion of a sample of water molecules in the models here reported, the simulations are not long enough to estimate reorganization energy (see for instance similar methods reported in the literature and references therein[22]). Nevertheless, our models provide snapshots of the most likely configurations along the pathway for Cu reduction. This information is mandatory for any further investigation of the redox chemistry of Cu in such systems.

The VMD program[23] was used for all the molecular drawings reported in the figures.

NOTATIONS

The PDB notation for atoms of the imidazole His side chain is used: Nδ (sometimes identified as Nπ) is N 3 in the imidazole-4-yl IUPAC notation for His side chain, and Nε (sometimes identified as Nτ) is N 1. The same notation is adopted for H atoms bonded to N atoms. The backbone amide atoms are identified as in the PDB, simply with N, H, C, and O. The N- and C-terminal capping groups, used in truncated peptide models, are acetyl and *N*-methylamide groups (indicated as Ac and NHMe, respectively).

RESULTS

At physiological pH, Cu(II) is bound in two different types of coordination, often called component I (major form: abbreviation **C1o**) and component II (minor form: abbreviation **C2o**), whereas only one form exists for Cu(I) in the pH range 6−9. Thus the reduction of Cu(II) to Cu(I) could occur from either form. To test this, we started with modeling **C2o**. A summary of the models described below and the associated chemical species is provided in Table 1.

Table 1. Summary of Models and Associated Chemical Species As Identified by Spectroscopy[a]

C2o	species consistent with component II (high pH, oxidized state)
	H_2N-**DA$^-$EFRHD**-NHMe + Cu^{2+} + 212 H_2O
C2r	species consistent with component II, then reduced
	H_2N-**DA$^-$EFRHD**-NHMe + Cu^{+} + Na^{+} + 211 H_2O
C3r	species consistent with component II, then protonated
	H_2N-**DAEFRHD**-NHMe + Cu^{2+} + Ac-**H**-NHMe + 281 H_2O
C1o	species consistent with component I (low pH, oxidized state)
	H_2N-**DAEFRHD**-NHMe + Cu^{2+} + Ac-**H**-NHMe + 267 H_2O
C1r	species consistent with component I, then reduced
	H_2N-**DAEFRHD**-NHMe + Cu^{+} + Ac-**H**-NHMe + Na^{+} + 266 H_2O

[a]Single-letter codes (boldface) are used for amino acids, and A$^-$ is the amide-deprotonated Ala residue.

C2o: Component II, the High-pH Cu(II)-Aβ Complex. Component II of Cu(II)-Aβ is the minor form at pH 7.4 but becomes predominant at pH ∼ 9.[17] Experiments suggest that Cu(II) is bound to NH_2 (Asp 1), N, and O (Ala 2) and to one His side chain.[24,25] We built a model of Cu(II)-Aβ(1−7) (**C2o**), with the C-terminus neutralized with a NH-methyl

dx.doi.org/10.1021/jp308977s | J. Phys. Chem. B 2012, 116, 11899−11910

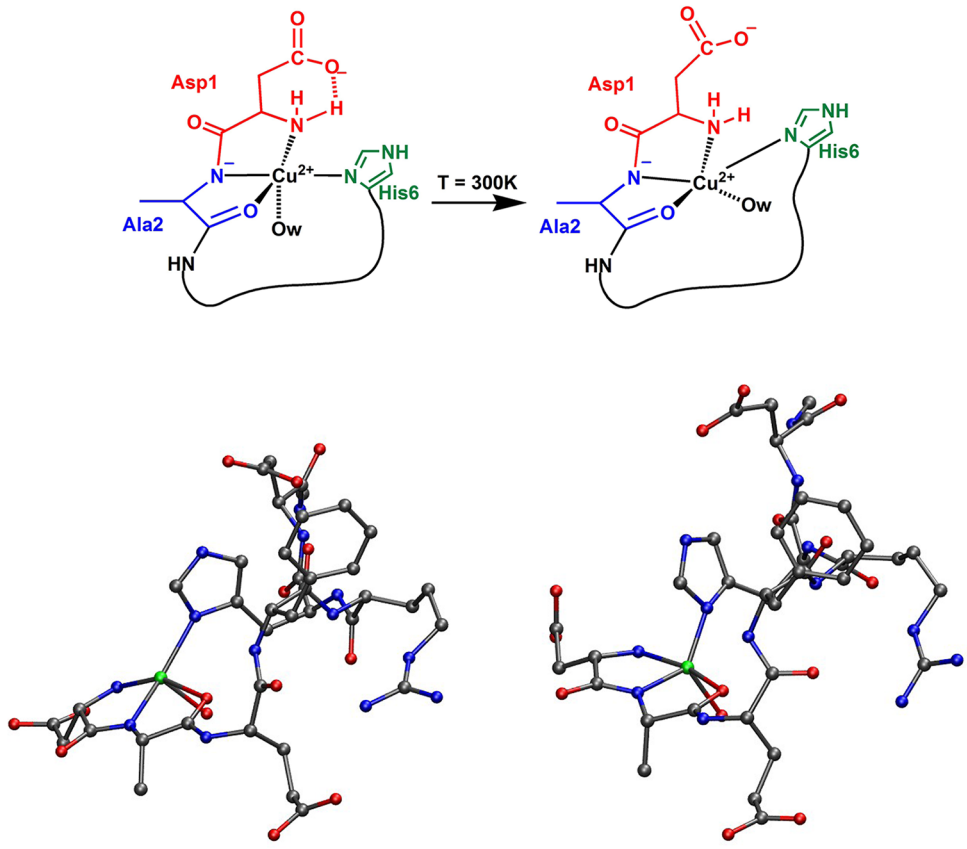

Figure 1. Schematic representation of high-pH model of Cu^{2+}-Aβ(1−7) (**C2o** model, top). Initial (energy minimized, bottom left) and final (t = 0.36 ps for CP-MD at T = 300 K, bottom right) configurations for the same model. Solvent water molecules are not displayed. Atomic radii are arbitrary, and the color scheme is gray for C, red for O, blue for N, and green for Cu.

Table 2. Summary of Distances (in Å) of the CP-MD Simulations at T = 300 K for the Five Models of Cu-Aβ Complex Investigated[a]

model	C2o	C2r	C3o	C1o	C1r
atom pair			distance		
N1−Cu	1.9−2.3	2.1−2.5	2.3−3.7	1.9−2.1	1.9−2.7
N2−Cu	1.9−2.1	1.8−2.1	3.6−4.2	3.9−4.6	3.8−4.7
O2−Cu	1.9−2.2	2.5−3.5	2.2−3.4	5.4−6.7	5.5−6.3
O1−Cu	4.8−5.8	5.0−5.4	5.4−6.0	1.9−2.6	1.9−2.6
N3−Cu	1.9−2.4	1.9−2.1	1.9−2.1	2.1−2.4	1.9−2.8
N4−Cu	=	=	1.8−2.1	1.9−2.3	1.9−2.3
Ow−Cu	1.9−2.3	–	2.0−3.0	1.8−2.6	–
Oδ1(D1)−N1	2.9−3.7	2.8−4.1	2.5−3.4	2.6−3.6	2.7−3.4
Oδ1(D7)−Nε(H6)	3.4−4.4	4.1−4.4	5.0−5.6	5.3−5.9	4.2−4.9
Oδ1(D1)−Nε(H13/14)	=	=	7.2−8.3	2.6−3.6	4.9−6.4
Cδ(E3)−Nζ(R5)	6.3−6.8	4.9−6.3	6.4−6.7	3.4−4.3	3.4−4.5

[a]Data are displayed as minimal−maximal range. Definitions for Cu first-sphere atoms: N1=N(Asp 1); N2=N(Ala 2); O2=O(Ala 2); O1=O(Asp 1); N3=Nδ(His 6); N4=Nδ(His 13/14); Ow=O (Cu-bound water molecule). When distances are larger than 2.5 Å and values are not bounded, values are not reported (dash). When atoms are absent in the model, an "=" symbol is reported.

group, to understand which interactions stabilize the Cu(II) coordination. The use of Aβ(1−7) is justified as it has been shown that Aβ(1−10), which contains neither His 13 nor His 14, shows the same spectroscopic signature of component II of Cu(II)-Aβ(1−16).[26] This is a suitable model because component I in Aβ(1−16) and Aβ(1−7) has the same Cu coordination sphere, including one His. The only difference is that in Aβ(1−16) the 3 His side chains are in fast exchange within the coordination sphere, whereas in Aβ(1−7) only His 6 is bound. Effects of residues His 13 and His 14 are introduced in the other models reported below. In these conditions, the oxidized form is stabilized, because the reduction of this form is not possible at potential smaller than −2 V, thus showing that no efficient mechanisms for Cu reduction are provided by the complex structure and dynamics. This experimental result shows that the high-pH complex acts as a reduction-silenced complex. The schematic model of **C2o**, i.e., Cu(II)-Aβ(1−7) is shown in Figure 1 (top).

The initial structure (represented in Figure 1, bottom left, as the energy-minimized structure resulting form the initial

dx.doi.org/10.1021/jp308977s | J. Phys. Chem. B 2012, 116, 11899−11910

construction) displays a square-base pyramidal coordination of Cu(II), with N(Asp 1), N(Ala 2), O(Ala 2), Nδ(His 6), and Cu(II) almost in the base plane, in line with the experimental information,[24] though EPR data are consistent with a more distorted coordination. In addition to the experimental information, a water molecule (Ow) is apically coordinated to Cu(II).

The configuration of the Asp 1 side chain is rather different from that suggested by NMR data at room temperature, where the possibility of an apical coordination of Oδ(Asp 1) to Cu has been proposed.[15] Even the construction of the initial model shows that an apical interaction of Oδ(Asp 1) with Cu(II) can be hardly imposed together with N(Asp 1) and N(Ala 2) coordination to Cu, because of the large propensity of the carboxyl Asp 1 group to interact with the NH_2 terminal amino group (see below). For this model, the temperature was increased to 300 K. Globally, the five ligands stayed bound to Cu(II), but the geometry changed.

Distances and angles averaged at T = 300 K (see Table 2 for distances and Table S2 (Supporting Information) for selected angles) show that Cu(II) is hosted in a distorted square-planar coordination site, with N(Asp 1), N(Ala 2), O(Ala 2), and Cu(II) in the plane and Nδ(His 6) and Ow significantly out of this plane (Figure 1, bottom right). The significant change of the initial coordination started at T > 50 K, with a significant decrease of the N(Ala 2)−Cu−Nδ(His 6) angle from the initial value of about 160° toward 90°. However, at T = 300 K, the N(Ala 2)−Cu−Nδ(His 6) angle increases from 106 to 132°, while the Nδ(His 6)−Cu−Ow angle was kept almost constant (109 ± 2°). The N(Ala 2)−Cu−Ow angle decreases from 141 to 112°. Therefore, a slight thermally induced rotation of the N(Asp 1)−N−O(Ala 2) plane (residues 1−2, wherein Cu is well kept in-plane) occurs with respect to a fluctuating Aβ(3−7) fragment. This movement tends to align the Nδ(His 6)−Cu bond in the N(Asp 1)−N−O(Ala 2) plane, as it is the case in the energy minimized structure (where angle N(Ala 2)−Cu−Nδ(His 6) is 158°). The peptide structure, however, opposes mechanical resistance against this alignment because of the right-hand topology of the peptide backbone, this latter favored by interactions between side chains. This topology does not allow the ideal alignment of the Nδ(His 6)−Cu bond with the N(Asp 1)−N−O(Ala 2) plane, thus weakening the His−Cu bond and strengthening the bond with a fifth ligand that can transiently fit in the same plane, in this case the Cu-bound water molecule (as it is shown by the simulation at T < 300 K).

The movement of the His 6 side chain out of the equatorial Cu-coordination plane reflects a significant propensity for Cu of exchanging His 6 with other His side chains in its coordination sphere also at high pH.[27] The force for such exchange can be provided by interactions occurring in N-terminal region of the Aβ peptide wrapped around Cu as suggested by experiments about component II. Indeed, several interactions within the peptide side chains favor the approximate right-hand topology described above. Some of them can be noticed by observing Figure 1 (bottom right). The most significant interaction is the Glu 3−Arg 5 nascent salt bridge. The Glu 3 side chain is kept away from the Cu coordination sphere by the Arg 5 side chain, through a fluctuating salt bridge commonly observed in simulations of the Aβ(1−16) region both in the vacuum[28] and in water solvent.[16] Despite the distance between Arg 5 and Glu 3 side chains displaying the largest maximal value among the simulated models (Table 2), the distance range is still consistent with a typical salt-bridge in proteins.[29] A second force that prevents the Glu 3 side chain from approaching Cu is the O(Ala 2)−Cu bond. Moreover, in Aβ, the Asp 7 carboxylate group tends to interact with the His 6 side chain via a hydrogen bond with Hε, as is usally the case in simulations of the 1−16 region.[16,28] Summarizing, the Glu 3−Arg 5 salt bridge and the Asp 7−His 6 hydrogen bond act as interactions that seal the right-hand helical wrapping of the peptide around Cu (Table 2). Asp 1 carboxylate is kept in the second coordination sphere of Cu by its interaction with the N-terminus of Asp 1, which is directly bonded to Cu.

At high pH, Asp 1 NMR signals are affected by Cu(II) addition,[25] thus showing either direct coordination of Asp 1 side chain to Cu or indirect interactions with Cu. The model here reported shows a stable six-membered pseudocycle H−N−Cα−Cβ−Cγ−Oδ (all atoms belonging to Asp 1) with N well coordinating Cu. The strong interaction between Oδ(Asp 1) and N(Asp 1), the latter directly bonded to Cu (Table 2), can explain an NMR broadening of the Asp 1 signals as an effect arising from the structural constraint forcing the Asp side chain in the N(Asp 1)−N−O (Ala 2) plane where also Cu lays (Figure 1, bottom right). However, a fast exchange between N(Asp 1) and Asp 1 carboxylate in the first-shell Cu coordination cannot be excluded by these calculations.

Summarizing, the distortion at T = 300 K of the hypothetical Cu coordination displayed in Figure 1 (bottom right compared to bottom left) and described above, is consistent with the propensity for an exchange among His 6 and His 13 or His 14, mediated by the labile water molecule here observed as moving within the Cu-coordination sphere.

C2r: Reduction of Component II, from C2o to C2r. In the following, the behavior of the reduction of the Cu(II) complex described above (component II, **C2o**), is summarized. The same initial structure of **C2o** was chosen: N (Asp 1), N(Ala 2), O(Ala 2), and N (His 6) bind Cu(I) in a square-base pyramidal coordination, with an apically Cu-bound water molecule. This complex mimics the behavior of the Cu-Aβ complex when it is reduced before proton addition to the solution.

Already at low temperature (T < 200 K), the O(Ala 2) atom moves far from Cu, reaching distances larger than 2.5 Å. At T = 300 K also the N(Asp 1)−Cu(I) bond starts to become weaker, as shown by the larger range spanned compared to the oxidized form (Table 2). H atoms of several water molecules approach N(Asp 1), showing the propensity for protons to replace the N(Asp 1)−Cu(I) interaction with a N(Asp1)−H bond. Together with the N(Asp 1)−Cu(I) bond weakening, the Cu(I)−Ow bond, still present in the local energy minimum, breaks, with the displacement of the initially Cu(II)-bound water molecule at distances larger than 3 Å. No other water molecules come at distances closer than 3 Å from Cu(I) at T = 300 K. The breaking of two bonds (O(Ala 2)−Cu and Ow−Cu) around Cu, together with the weak interaction of Cu with N(Asp 1), produces a distorted T-like N(Ala 2)−Cu-Nδ(His 6) coordination perturbed by N(Asp 1). The extent of the distortion (the N(Ala 2)−Cu−Nδ(His 6) angle is 158 ± 5° at T = 300 K) away from the linear geometry, together with the larger N(Ala 2) exposure to water solvent, indicates a larger chance of N(Ala 2) protonation by water compared to the Cu(II) (oxidized) state. In the oxidized state water molecules eventually approaching backbone N atoms are diverted toward the apical Cu(II) open coordination, whereas this effect is not observed in the reduced state. Once the N(Asp 1) or N(Ala 2) protonation occurs, the chance for the release of Cu from the

peptide into water becomes larger if no other His side chains are in the nearby. Moreover, the protonation of N(Asp 1) after moving the N-terminus away from Cu(I), enhances the chance for the positively charged N-terminus to seize the carboxylate of Asp 1, hindering its possible interaction with Cu and removing it from the list of potential Cu(I) ligands alternative to His.

It is interesting to notice that, in the reduced form, although the Glu 3-Arg 5 side chains can become slightly closer than in the oxidized form (Table 2), they are still too far for a proper hydrogen bond. The hindrance to form a stronger interaction compared to the salt bridge, is likely because when O(Ala 2) moves away from Cu(I), the peptide backbone relaxes only partially the stress initially induced by O(Ala 2)-Cu bond, and O(Glu 3) is still perturbing the side chain of Arg 5 (Figures 1 and 2).

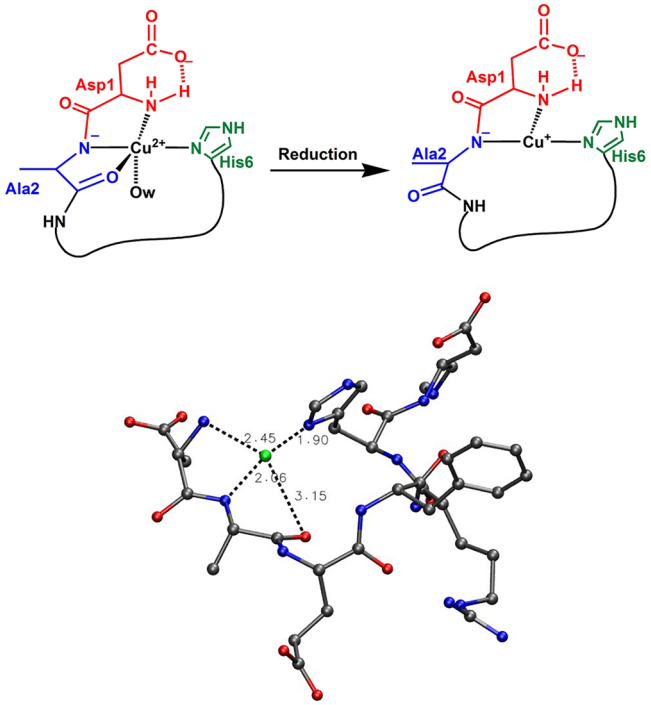

Figure 2. Schematic representation of high-pH reduction of Cu(II)-Aβ(1−7) component II (**C2o**, top left) yielding the Cu(I) complex (**C2r**, top right). Final (t = 0.27 ps for CP-MD at T = 300 K) configuration of model **C2r** (bottom). See Figure 1 for the drawing scheme.

C4o: The Approach of His 13 or His 14 to Cu(II) in Component II (C2o) Is Not Possible. In the previous section, the reduction of component II, **C2o**, to **C2r** resulted in a partially decomposition of the complex. As in the most stable Cu(I)-Aβ complex, Cu(I) is bound to two His (mainly His 13 and His 14), the approach of a second His belonging to the pair 13−14 might be crucial for an efficient reduction of Cu(II). Therefore, a possible model mimicking the Cu(II)-Aβ(1−16) component II, with Cu(II) interacting also with the His13−His14 region, has been built as explained in the Methods (see Supporting Information).

The low temperature simulation (T = 50 K, data not shown) shows that the Cu(II) ion is rapidly moved away from the Nδ atom of the added His 13 model, with a complete reconstruction of the coordination observed in the previous Cu(II)-Aβ(1−7) model (**C2o**) (Figure 3). The final Nδ(His 13)−Cu(II) distance is 2.4 Å, but Cu(II) is far from the imidazolyl plane of His 13, although it is still well kept in the imidazolyl plane of His 6, this latter side chain being able to follow the Cu(II) movement toward the N(Ala 2) atom. The apical location of a second His, His 13 introduced into the high-pH coordination site of Cu(II), is, therefore, not prone to form bonds with Cu(II), whereas the first His, His 6, closer to the N(Asp 1)−N−O(Ala 2) plane, is still able to efficiently interact with the Cu(II) site. The major difference between this simulation and the simulation of the previous N-terminal site (**C2o**), is that no water molecules enter into the Cu(II) coordination sphere after the movement of His 13/14 away from Cu(II). This occurs mainly because of the steric hindrance of the segment containing, in this model, His 13, which, even when Cu(II)-unbound, displaces water molecules away from the nearby of Cu(II).

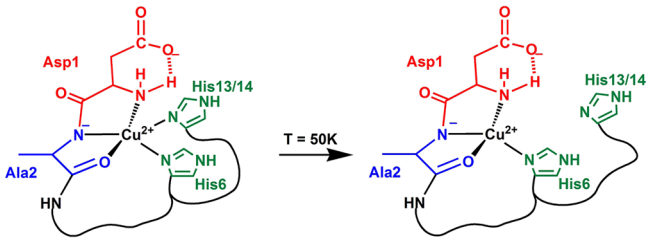

Figure 3. Schematic representation for the approach of His 13 to Cu in the high-pH Cu^{2+}-Aβ(1−7) state **C2o** (the **C4o** model), going back to the **C2o** state (Figure 1, top).

C3o: Binding of His 13 or His 14 to Cu(II) in Component II (C2o) Is Possible after Protonation of N(Ala 2). A key feature upon passsing from component II to component I, which are in fast equilibrium at neutral pH, is the protonation of N(Ala 2). Therefore, we wanted to investigate if the approach and binding of His 13/14 is possible when N(Ala 2) is protonated. Indeed, the protonation of N(Ala 2) drastically changes the time evolution after His is introduced into the Cu(II) coordination sphere.

In this case the Cu(II) ion is well kept within the two Nδ atoms of His 6 and His 13 up to T = 300 K. The final geometry is a rhombic-distorted square-planar Cu(II)-coordination by O(Ala 2), Nδ(His 6), Nδ(His 13), and the O of a water molecule (Ow). The two longer bonds are respectively with O(Ala 2) and Ow (Figure 4, bottom, and Table 2). The N(Asp 1) atom moves at a distance larger than 3 Å from Cu (Table 2) and the water molecule enters into the Cu coordination sphere at the same time N(Asp 1) exits. The water molecule enters anti with respect to O(Ala 2), while N(Asp 1) exits from a direction that is axial to the nascent square-planar coordination. This rearrangement of ligands around Cu preserves an approximately square-base pyramidal coordination through a movement that, once N(Ala 2) is protonated, consists simply of the N(Asp 1) exchange with a water molecule around Cu. Noticeably, this water molecule could enter into Cu coordination sphere despite the possible hindrance due to the His 13/14 segment.

When this simple rearrangement is completed, the final coordination (Figure 4 bottom right) becomes very similar to the coordination observed for Cu(I) in Aβ, with the His 13−Cu−His 14 coordination replaced, in this case, by His 6-Cu−His 13. The His 13−His 14 dyad has statistically larger chance than the His 6-His 13/14 pair to form the linear coordination without imposing significant distortions to the Aβ(1−16)

dx.doi.org/10.1021/jp308977s | J. Phys. Chem. B 2012, 116, 11899−11910

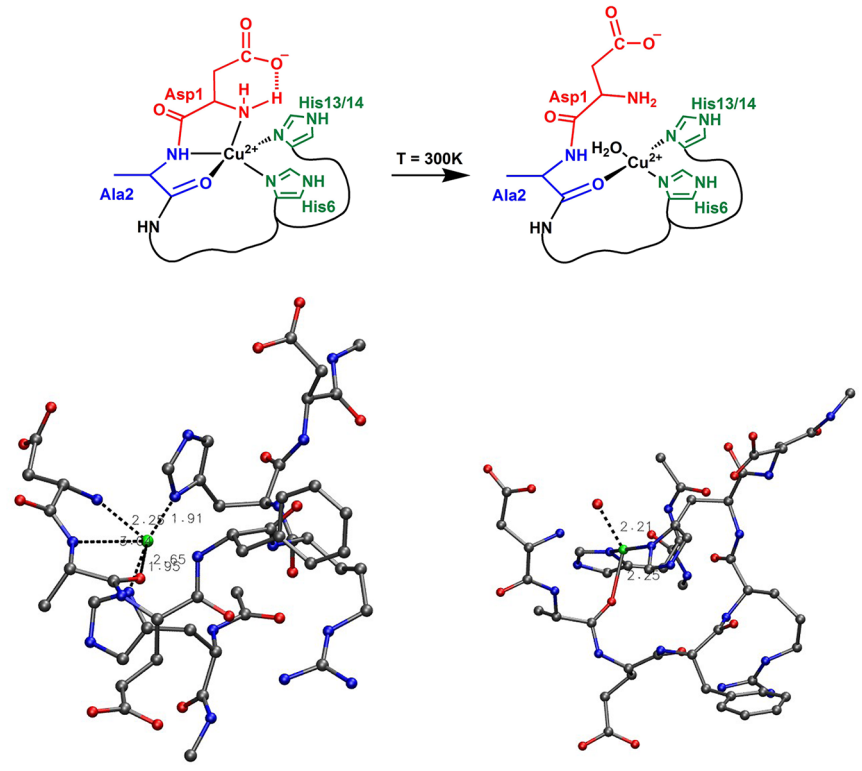

Figure 4. Schematic representation (top) for the approach of His 13 to Cu in the low-pH Cu^{2+}-Aβ(1−7) state, first model (**C3o**). The low pH condition is introduced via the protonation of the amidyl function bound to Cu(II) in Ala 2 of **C2o**. Dashed lines represent weaker bonds. Initial (t = 0.12 ps at T = 50 K, bottom left) and final (t = 0.26 ps for CP-MD at T = 300 K, bottom right) configurations for the same model. Only water molecules interacting with Cu are displayed. See Figure 1 for the drawing scheme.

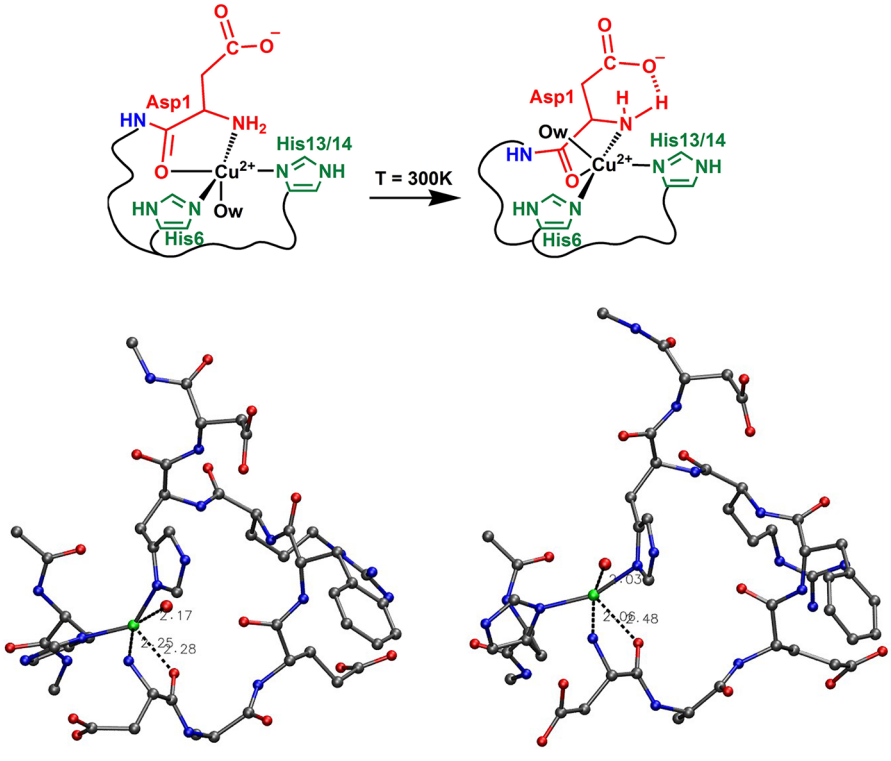

Figure 5. Schematic representation (top) for the approach of His 13 in the low-pH Cu^{2+}-Aβ(1−7) state, second model (**C1o**). Initial (t = 0.12 ps at T = 50 K, bottom left) and final (t = 0.22 ps for CP-MD at T = 300 K, bottom right) configurations for the same model. See Figure 1 for the drawing scheme.

dx.doi.org/10.1021/jp308977s | J. Phys. Chem. B 2012, 116, 11899−11910

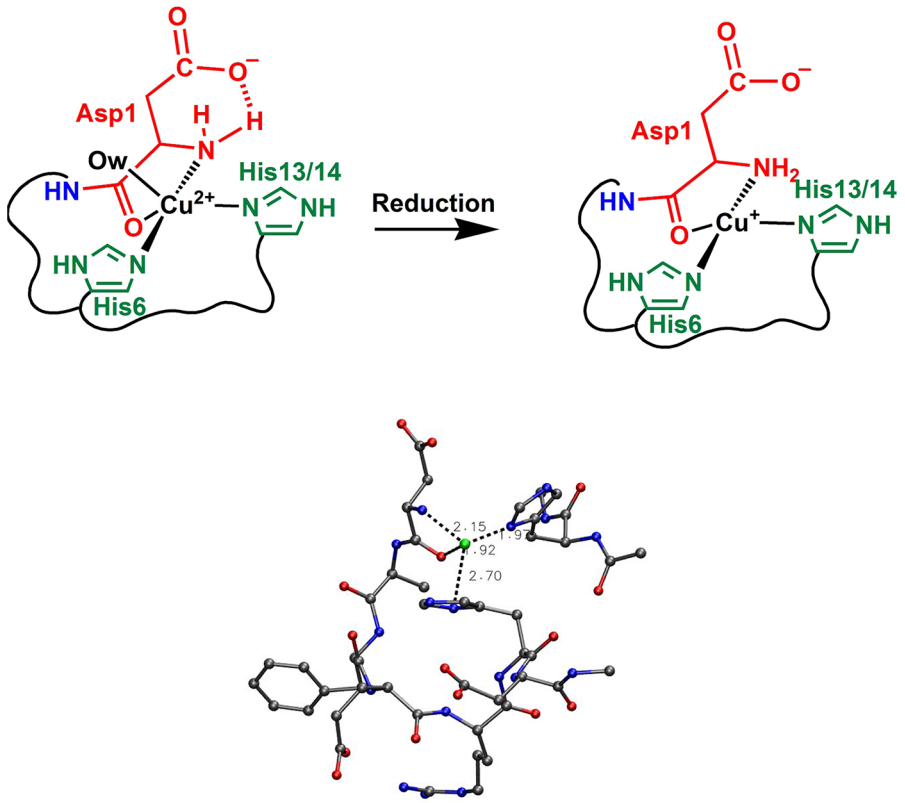

Figure 6. Schematic representation for the reduction of **C1o** model in the low-pH Cu^{2+}-Aβ(1−7) state (**C1r** model). Final (t = 0.38 ps for CP-MD at T = 300 K) configuration for the same model (bottom). See Figure 1 for the drawing scheme.

chain.[16] However, in this case the Aβ(1−16) chain with His 6 and His 13 bonded to Cu(I) is assisted by O(Ala 2) and by a water molecule. Because the O(Ala 2)−Cu bond is slightly elongated at room temperature, the further exchange of His 6 with the second His of the 13−14 pair, assisted by carbonyl groups belonging to the same pair, appears favored.

C1o and C1r: Reduction of Component I of Cu(II)-Aβ. After exploring the reduction of component II (see above model **C2r**), which showed that reduction is not favored without a significant rearrangement of Cu first-coordination sphere, we investigated whether component I is more likely to be reduced. Before tackling the reduction, the model was built and its evolution monitored.

C1o: Evolution of Component I of Cu(II)-Aβ. This model mimics the component I identified by experiments.[24,25,27]

The initial coordination of Cu is to N(Asp 1), O(Asp 1), Nδ(His 6), and Nδ(His 13). The exchange of O(Ala 2) with O(Asp 1) in the Cu first coordination sphere mimics a possible krankshaft motion of the peptide backbone that becomes available once N(Ala 2) is protonated and not constrained by the N−Cu bond. With respect to Cu, this rearrangement of the peptide backbone consists of the replacement of the five-membered ring Cu−N−Cα−C−O−Cu, with backbone atoms belonging to Ala 2, with the same kind of ring with atoms belonging to Asp 1.

The comparison between the initial and final configurations obtained by simulating this model (Figure 5, bottom), shows that the initial coordination is, in this case, kept up to room temperature. The coordination holds a distorted square-base pyramidal geometry, with N(Asp 1), Nδ(His 6), Nδ(His 13), and a water molecule (Ow) in the plane and O(Asp 1) apically bonded to Cu (Table 2 and Table S2, Supporting Information). The Cu−O(Asp 1) distance is elongated up to 2.6 Å, a maximal distance similar to that adopted by the Cu−Ow bond. The five-membered ring formed by Asp 1 is almost perpendicular to the Nδ(His 6)−Cu−Nδ(His 13) plane, where also the water molecule is approximately located. The salt bridge between Arg 5 and Glu 3 is kept during the simulation and it is at a closer distance than in the **C2** models. Other long-range interactions affect the stability of the Cu coordination and are absent in the first low-pH model **C3o**. One of these interactions is that between the Asp 1 carboxylate group and Nϵ(His 13) (Table 2). Because of this array of interactions in the second Cu-coordination shell, residues Asp 1, Glu 3, Arg 5, and Asp 7 all contribute to the Cu binding, keeping the entire N-terminus wrapped around Cu also when the external His side chain (His 13) enters into the Cu coordination sphere.

C1r: Reduction of Component I of Cu(II)-Aβ(1−16). The final configuration obtained by CP-MD of component I of Cu(II)-Aβ complex was then reduced. This lead to significant changes in the Cu coordination sphere. During the heating up of the system (T < 300 K) the Cu(I) ion appears attracted within the two His side chains. The Nδ(His 6)−Cu−Nδ(His 13) angle is kept at about 140°, the Cu(II)-bound water molecule (present in the oxidized state) is kept coordinated to Cu(I) and the N(Asp 1) and O(Asp 1) atoms appear weakly interacting with Cu(I). This coordination resembles that displayed by the reduced stable form of Cu-Aβ complex,[16] with Cu(I) well kept within His 13 and His 14 side chains and one or two ligands weakly perturbing an almost digonal coordination.

When the system reaches the room temperature (T = 300 K), this coordination is changed: both the Nδ(His)−Cu bonds become distorted and the N(Asp 1) atom becomes more

dx.doi.org/10.1021/jp308977s | J. Phys. Chem. B 2012, 116, 11899−11910

tightly bound to Cu compared to the Nδ atoms of His. The water molecule initially bonded to Cu moves away from the Cu coordination sphere and no water molecule replaces it. The fluctuating hydrogen bond between N(Asp 1) and Oδ(Asp 1) is kept at T = 300 K (Table 2). The increase of the N(Asp 1)−Oδ(Asp 1) distance (data not shown) is approximately in phase with the increase of the N(Asp 1)−Cu distance. This confirms that the N(Asp 1)−Cu bond is rapidly activated by the N(Asp 1)-Oδ interaction. The result of this change is represented in Figure 6, where the final configuration obtained by CP-MD at T = 300 K is displayed. Comparing this structure with that displayed in Figure 2 (bottom), it can be noticed that the 3−7 region in **C1r** is more extended away from Cu than in **C2r**, because of the release of the His 6 side chain from the first Cu-coordination sphere. The stronger interaction between Oδ(Asp 1) and Nε(His 13) (Table 2), together with all the Cu second-sphere interactions, shows that N(Asp 1) may be transiently inactivated for the Cu binding and it may be easily exchanged with another ligand like a third approaching His side chain (His 14). Therefore, this structure can represent a reduced intermediate state (like **C3o** is in the oxidized state) toward a more stable His 13−Cu(I)−His 14 binding site, like that observed in the previous modeling of Cu(I)-Aβ complex.[16] Thanks to the two Oδ oxygen atoms of the Asp 1 carboxylate side chain, the Asp 1 pseudocyclic ligand may act as a chaperon of His 13 side chain for the exchange between His 6 and His 14 as Cu ligands.

Truncated Models in the Vacuum. The short MD simulations above gave very intriguing insights into the redox reactions of Cu-Aβ, the underlying mechanism of ROS production. They revealed possible pathways for the large structural rearrangement upon reduction and suggested that the protonation state of N(Ala 2) is key for reduction. To estimate energy differences between the different models and to dissect the effects of peptide mechanics from the coordination chemistry of Cu, the His side chains were separated as 4-methylimidazole molecules (MeIm, hereafter) and the 1−7 peptide of the CP-MD simulations was truncated to the Asp-Ala-NHMe segment. Only the water molecules potentially bound to Cu, as indicated by the solvated CP-MD models, were kept in the truncated models. Water molecules not binding Cu in the truncated models (distance larger than 2.5 Å in the energy-minimized structure) are removed from the model for the final electronic structure calculation. Distances between selected atoms, the extent of electron sharing between atom pairs (delocalization indices, δ), and the charge associated to atomic basins (q) are reported in Table 3 to summarize coordination geometries and the associated electronic structures (see also Table S3, Supporting Information, for more details).

*Truncated Component II (**C2o**).* In the truncated model **C2o** the water molecule identified in CP-MD simulation does not bind Cu and the Cu coordination reaches the square-planar coordination with N(Asp 1), N(Ala 2), O(Ala 2), Nδ(His 6), and Cu in the same plane identified in the initial local minimum by CP-MD (Figure 1, bottom left). This observation confirms the mechanical constraint exerted by the 1−7 peptide chain, where, at room temperature, the water molecule is kept Cu-bound in the N(Asp 1)−N−O(Ala 2)−Cu plane, while His 6 is forced to be more oriented toward the plane axis (Figure 1, bottom right). The arrangement obtained by truncation is still consistent with the strong hydrogen bond between the carboxylate group of Asp 1 and N(Asp 1). This latter interaction is also witnessed by the significant delocalization index between Oδ and N of Asp 1 (δ = 0.36), which is the largest value measured for this pair among all the truncated models.

Table 3. Summary of Geometry and Electronic Structure for the Different Truncated Models Investigated by Energy Minimization[a]

model	C2o	C2r	C3o	C1o	C1r
atom pair			distance		
N1−Cu	2.07	2.06	–	2.09	2.16
N2−Cu	1.92	1.98	–	–	–
O2−Cu	2.19	–	–	–	–
O1−Cu	–	–	–	2.46	-
N3−Cu	1.99	1.92	1.95	2.00	1.97
N4−Cu	=	=	1.95	2.01	1.98
Ow-Cu	=	=	1.97	2.29	=
Oδ1-H1	1.52	1.60	–	1.56	1.74
geometry	square-planar	trigonal	T	square pyramidal	T
atom pair			δ		
N1−Cu	0.53	0.66	–	0.48	0.53
N2−Cu	0.64	0.67	–	–	–
O2−Cu	0.34	–	–	–	–
O1−Cu	–	–	–	0.21	0.15
N3−Cu	0.59	0.79	0.74	0.56	0.72
N4−Cu	=	=	0.75	0.61	0.69
Ow−Cu	=	=	0.64	0.31	=
Oδ1−N1	0.36	0.32	–	0.35	0.25
atom			q		
Cu	0.88	0.64	0.74	0.97	0.68
N1	−0.22	−0.30	−0.28	−0.17	−0.28
N2	−1.2	−1.1	−0.74	−0.67	−0.69
O2	−1.3	−1.0	−1.3	−1.3	−1.3
O1	−1.0	−1.1	−0.96	−1.2	−1.2
N3	−1.1	−1.1	−1.2	−1.1	−1.1
N4	=	=	−1.1	−1.1	−1.2
Ow	=	=	−0.59[b]	0.05[c]	–
Oδ1	−1.1	−1.2	−0.53[b]	−1.2	−1.1
Oδ2	−1.2	−1.3	−1.2	−1.3	−1.0
E	0	−673	−88	−119	−1056

[a]Distances are in Å, delocalization indices (δ) and atomic charges (q) are in the number of electrons (see text for details). When distances are larger than 2.5 Å and delocalization indices are smaller than 0.1, values are not reported (dash). When atoms are absent in the model, an "=" symbol is reported. Hydrogen atoms bonded to more electronegative atoms (like in NH2 groups) belong to the heavy atom basin. N1═N(Asp 1), N2═N(Ala 2), O2═O(Ala 2), O1═O(Asp 1), N3═Nδ(His 6), N4═Nδ(His 13/14), Ow═O(water), Oδ1═Oδ(Asp 1) closest to N1, H1═HN(Asp 1) closest to Oδ1. [b]O is hydroxide and Oδ1 is protonated. [c]q(O) in isolated water is zero, the protons being in the same atomic basin of O. E (last row) is in kJ/mol.

*Truncated Reduced Component II (**C2r**).* Upon reduction (truncated **C2r**), the coordination of Cu becomes almost trigonal, with the two tight N(Ala 2)−Cu and Nδ(His 6)−Cu bonds perturbed by N(Asp 1). This shows that there are no significant mechanical constraints perturbing the structure obtained by CP-MD (Figure 2, bottom) when O(Ala 2) is expelled away from the first Cu-coordination sphere. The backbone movement following this coordination change assists the His 6 settling in the reduced Cu site.

*Truncated Component II with Protonated N(Ala 2) and Close-by His (**C3o**).* Once the His 13 moiety is introduced at low pH (N(Ala 2) is protonated, truncated **C3o** model), Asp 1 is expelled away from the second Cu-coordination sphere and the Cu coordination adopts a T-like geometry, with two linear Nδ(His)−Cu bonds perturbed by a water molecule strongly activated by the Asp 1 side chain. It is interesting to notice that the charge of the Cu basin becomes more similar to a reduced state (**C2r** and **C1r**) than to the other oxidized states (**C2o** and **C1o**). This means that the positive charge is more sparsed on the peptide ligand than on the Cu hole. The energy difference between **C3o** and **C2o** is −88 kJ/mol, which is less negative than that obtained for **C1o** (−119 kJ/mol). The other energy values, all with **C2o** as energy reference, are reported in Table 3.

*Truncated Component I (**C1o**).* The energy minimization of the truncated **C1o** model provides almost the same geometry displayed at the end of the CP-MD simulation (Figure 5, bottom right). The atoms N(Asp 1), Nδ(His 6), Nδ(His 13), and O of a water molecule are tightly bonded to Cu in a distorted square-planar geometry, with the four coordination angles in the range 85−99°. Atom O(Asp 1) is interacting in the axial position almost via an electrostatic interaction (d = 2.5 Å). The plane formed by the Asp 1 residue (still strongly involved in the hydrogen bond with N(Asp 1)) is almost parallel to the plane of the His 13 side chain, while the two His side chains (the two MeIm planes in the truncated models) form an angle of about 45°, a value consistent with what observed in the stable reduced Cu-Aβ(1−16) complex.[16]

*Truncated Reduced Component I (**C1r**).* Upon reduction, the truncated C1r model behaves differently compared to the CP-MD model. The formation of a minimal energy T-like geometry is not hindered by the peptide constraints and the Nδ(His 6)−Cu−Nδ(His 13) angle can adopt a value of 143°, whereas in CP-MD the value fluctuates within 95 and 140°. The Oδ−N(Asp 1) interaction becomes weak (distance becomes 1.74 Å; see Table 3) because the Hε of His 13 approaches one of the two Oδ atoms of Asp 1. This confirms the second possible role played by the carboxylate group of Asp 1 in the second Cu-coordination sphere, an effect also observed in CP-MD simulation (Table 2). The movement of the His 13/14 side chain associated with the increase of the Nδ(His 6)−Cu−Nδ(His 13) angle is not observed in CP-MD, where Cu is partially diverted from the His 6 binding (Figure 6). Nevertheless, in the CP-MD simulation the perturbation of the Asp 1 pseudocycle is still operated by Nε of His13/14. Noticeably, the charges of Cu in **C2r** and **C1r** are similar, whereas in the oxidized forms there is a larger difference in polarization between Cu and the ligands (mainly related to the apical O(Asp 1) ligand in **C1o**). Despite the larger polarization (q(Cu) = 0.97 in **C1o** and 0.88 in **C2o**, respectively), **C1o** is energetically favored compared to **C2o** of about 120 kJ/mol in the vacuum.

The energy contribution (Table 3) for the transformation of the high-pH oxidized complex (**C2o**) into the low-pH reduced form (**C1r**), is dominated by the reduction at low pH. The direct reduction of **C2** is less energetically favored than that of **C1** (−673 compared to −1056 kJ/mol).

In general, the main differences between Cu(II) and Cu(I) coordination concern the involvement of the N-terminal amino acids (Asp 1−Ala 2) in the oxidized state but not in the reduced state. In other words, upon reduction the segment Asp 1−Ala 2 leaves the Cu first coordination sphere. In this context, it is interesting to note that the strong interaction between COO^- and NH_2 of Asp 1 with Cu is kept in the reduced form of **C2** and it hinders the release of COO^- of Asp 1 from the second Cu-coordination sphere in the reduced form. This barrier acts as a further frustration for the binding of Cu by His 13 or 14 in the **C2** (N(Ala 2) deprotonated) form. The indirect interaction of Asp 1 side chain COO^- with Cu (via NH_2 of Asp1) is less active in the reduced form of **C1**, where Oδ (Asp 1) is in the position to interact with the approaching His 13/14 moiety. The release of Asp 1 may be important in stabilizing alternative reduced forms of the Cu-Aβ complex, because the interaction between Asp 1 and His 14 has been observed as a persistent interdomain interaction in the most stable form of the reduced complex.[16] This is in line with an easier release of Asp 1 (both COO^- and NH_2) from Cu(I) in **C1r** compared to **C2r**, a prerequisite to reach the His−Cu(I)−His coordination, which is the most stable Cu(I)-Aβ structure.

Another factor influencing the different reduction behavior is the C═O bound to Cu(II). In the reduction of **C2** the bound C═O from Ala 2 moves away from Cu(I), whereas in **C1** the bound C═O from Asp 1 is weakly interacting with Cu. This constrained orientation of the C−O bond of Asp1 reduces the reorganization energy, by keeping the region between Ala 2 and His 6 more rigid, together with the contribution of the salt-bridge between Arg 5 and Glu 3 side chains. This latter salt bridge is stronger in the **C1** forms, thus assisting the N(Ala 2) protonation also in the presence of a nearby Cu^{2+} (not yet reduced) ion. Again, this interaction points to a lower reorganization energy in component I (**C1o**) and it should facilitate the reduction compared to component II.

Another interesting feature is the binding of water to Cu. Water binding to Cu indicates an accessible coordination site, to which also a reducing agent could coordinate, as would be the case when a first coordination sphere (inner-sphere) reduction of Cu(II) occurs. The attraction between Cu(II) and a water molecule in the truncated model of **C1** when this latter is oxidized (Figure 5, bottom right), shows that the proximity of a potential reducing agent (in place of a solvent water molecule) is more favored in this state than in the oxidized **C2** species. Indeed, in this latter state the water molecule, which is observed in the CP-MD simulation, is released upon energy minimization in the vacuum. However, it is a general feature of all the oxidized models to attract one water molecule around Cu, whereas none of the reduced models has this feature. The more hydrophobic character of the reduced forms can assist the formation of the cleft between the 1−8 and 9−16 domains observed in models of the reduced complex.[16]

CONCLUSION

First−principles molecular dynamics of several constructs for the Cu-amyloid β complex, inspired by experiments performed for the monomeric soluble species, have been performed and described in the two possible oxidation states for Cu. The models were simulated for short times to assess the proposed Cu coordination in a sample of liquid water at room temperature and density. The results of the simulations were completed with simpler truncated models energy-minimized in the vacuum. The electronic structure of these models was investigated by means of delocalization indices, measuring the extent of electron sharing in covalent bonds, and of atomic charges.

The combination of detailed and simple models provided a dissection of first- and second-sphere interactions in the

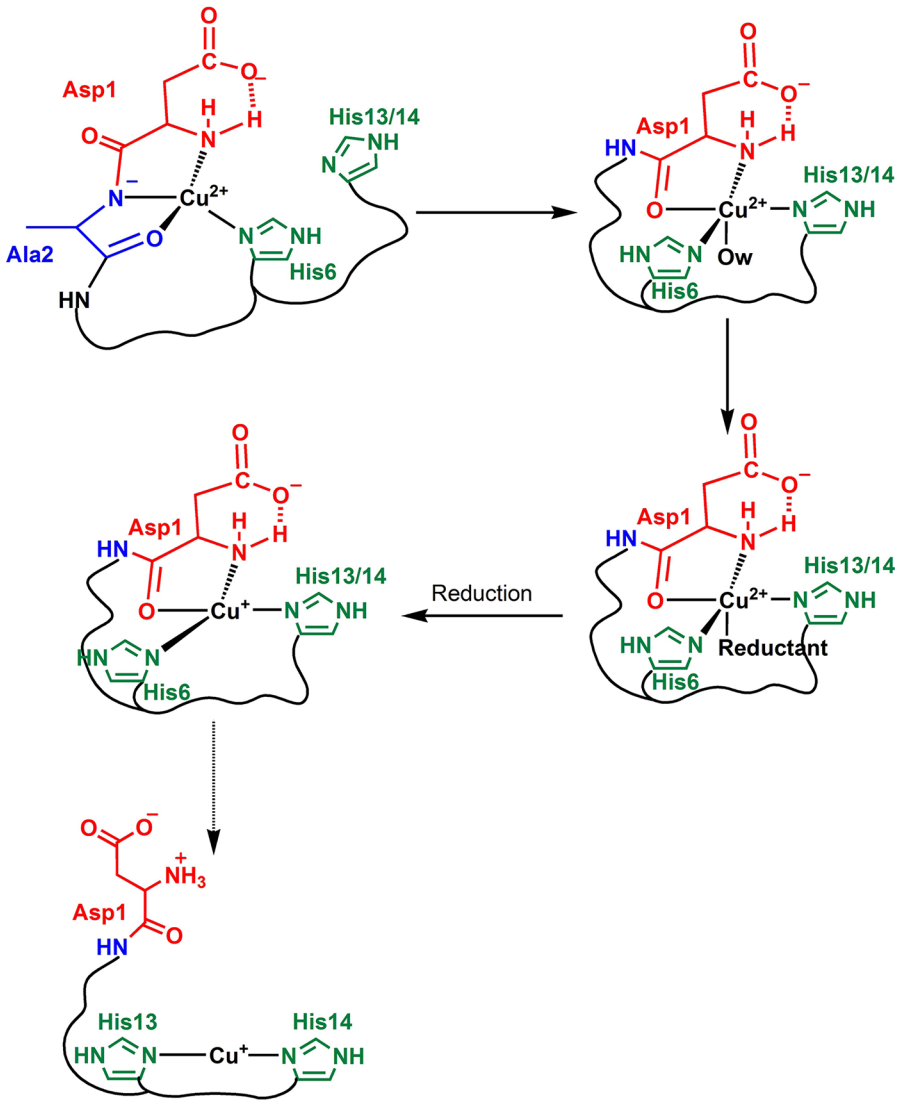

Figure 7. Summary of the proposed mechanism for Cu-Aβ reduction.

monomeric Cu-Aβ complex. The side chain COO^- of Asp 1 plays an important role in the coordination of Cu in all the calculations performed. The role is an electrostatic interaction that in certain cases provides to the carboxylate the role of a hydrogen bond acceptor of the Cu-bound N-terminal NH_2 group of Asp 1. As such, Asp 1 forms a six-membered pseudocycle, stabilized be the hydrogen bond between COO^- and NH_2. This interaction strengthen the bond of NH_2 (Asp 1) with Cu(II). The calculations suggest that a direct binding of the carboxylate group of Asp 1 to Cu(II) is incompatible with a simultaneous Cu(II)-binding of the N-terminal amino group of Asp 1.

The results obtained suggest that the reduction of Cu(II)-Aβ at high pH (component II) is energetically less favored than that of Cu(II)-Aβ in the low pH state (component I). Component II seems to be sluggish in the Cu reduction, because the approach of a second His side chain (13 or 14), which is known to stabilize the reduced form, cannot displace the amidyl N−Cu bond (N(Ala 2)−Cu). This is due to the contribution to complex stability of the charged amidyl group when no excess protons are provided by the environment. Moreover, the N−Cu bond is assisted by the other contributions: chelation by the Asp 1−Ala 2 fragment and Nδ(His 6)−Cu bond in anti to the N(Ala 2)−Cu bond, similarly to the prion N-terminal binding site.[30]

The importance of the N (Ala2)−Cu bond for the Cu reduction, was supported by the modeling of component II after protonation of N (Ala2). In this state, where only one His is bound, the approach of a second His in the first Cu(II)-coordination sphere was possible. Several second-sphere interactions contributed to the approach. Among these interactions, the Glu 3−Arg 5 salt bridge and the hydrogen bond between Asp 1 and His 13/14 side chains were the most evident. These interactions assisted the shuttling of Cu from His 6 to His 13 binding, once the His 13−His 14 segment is allowed to enter into the Cu-coordination sphere. The shuttling occurs with a small rearrangement of the pseudocycle formed by the Asp 1 side chain. With the presence of His 13/14 in the first Cu-coordination sphere, the reduction of Cu(II)-Aβ is less frustrated and more energetically favored compared to component II.

These data support the finding that the reduction of Cu(II)-Aβ at physiological pH (where a mixture of components I and II is present in solution) is sluggish. Component I is more favored than component II for reduction, suggesting that reduction starts with component I rather than with component

II. Thus, the following mechanism for reduction of Cu(II)-Aβ over a physiological pH range (6−9) can be proposed (Figure 7) for component II: (i) protonation of N (Ala 2); (ii) reshuffling of Asp 1 and Ala 2 around Cu(II), concerted with the His 13/14 approach to Cu(II); (iii) replacement of the Cu(II)-bound water by the reducing agent; (iv) reduction of Cu(II) to Cu(I); (v) shuttling of reduced Cu(I) from the N-terminal site toward the His 13−His 14 pair. In the case of component I, the mechanism consists of points iii−v.

Recent electrochemical measurements suggested a preorganized electron transfer mechanism, with a low populated entatic state where fast reduction occurs. This hypothetical state might well be provided by configurations sampled along the **C1o** reduction to **C1r**. It is more likely on this path than on the alternative low-pH reduction pathway going through **C3o**, because the latter state is characterized by a wide motion of C═O in Ala 2 and it is hence expected to have a much larger reorganization energy than the preformed **C1o** species.

The reduction and reoxidation of Cu(II)-Aβ is the underlying mechanism of ROS production in the presence of a physiological reducing agent, a process that has been suggested to contribute to the oxidative stress observed in Alzheimer's disease. Thus inhibiting this redox process has been considered as a potential therapeutic strategy. Classically, the approaches included the use of a copper chelator that is able to withdraw Cu from Aβ.[31−33] To not contribute to ROS production, the chelator has to be designed to have the proper affinity and to redox silence Cu.

An alternative approach would be to redox-silence the Cu bound to Aβ. A possibility would be to lock the Cu(II)-Aβ in the component II state, as the present studies suggest a more sluggish reduction in this state. However, this lock should be complete, because the fast exchange with component I allows the reduction. Hence a shift to a higher population of component II (as it occurs with a rise in pH) might be not enough. Another possibility, based on the above results, would be hindering the approach of His 13 and His 14 toward Cu(II). This might be obtained by blocking these His pair from binding to Cu(II), for instance with a Pt compound.[34,35] It would be important to block specifically both His (i.e., His13 and 14), as one seems to be enough to bind to Cu(II) and favor the reduction. Other strategies to hinder the approach of His13/14 can be imagined, for instance the cleavage of Aβ between His 6 and His 13.

■ ASSOCIATED CONTENT

Supporting Information

Section describing the details of the computational procedure used for building the initial atomic configurations of each model and for the Car−Parrinello molecular dynamics simulations performed. Table S1 reports time and temperature for the different stages. Table S2 reports details about the geometry of the simulated models, and Table S3 reports the same data for relaxed models in the vacuum. This material is available free of charge via the Internet at http://pubs.acs.org.

■ AUTHOR INFORMATION

Corresponding Author

*E-mail: glapenna@iccom.cnr.it.

Notes

The authors declare no competing financial interest.

■ ACKNOWLEDGMENTS

This work has been performed with resources provided by the following high-performance computing infrastructures: IDRIS and CINES (France, project n. i2010086191, year 2010); CALMIP (France, project n. P1049, year 2010); CINECA (Italy, project n. HP10B3VCG6, year 2010). S.F. contributed to this work under the Marie Curie intraeuropean fellowship FP7-PEOPLE-IEF-2008 (project nr. 237651, "MetAlzComp - Understanding the role of transition metals in Alzheimer's disease on a molecular level"). Funding for exchange of researchers came from the bilateral CNR (IT)-CNRS (FR) 2012-2013 programme. The authors thank Prof. M. Caffarel and Dr. A. Scemama (Univ. of Toulouse, FR) for the helpful discussions.

■ REFERENCES

(1) Kaplan, J. H.; Lutsenko, S. *J. Biol. Chem.* **2009**, *284*, 25461−25465.
(2) Robinson, N. J.; Winge, D. R. *Annu. Rev. Biochem.* **2010**, *79*, 537−562.
(3) Finney, L. A.; O'Halloran, T. V. *Science* **2003**, *300*, 931−936.
(4) Delangle, P.; Mintz, E. *Dalton Trans.* **2012**, *41*, 6359−6370.
(5) James, S. A.; Volitakis, I.; Adlard, P. A.; Duce, J. A.; Masters, C. L.; Cherny, R. A.; Bush, A. I. *Free Radic. Biol. Med.* **2012**, *52*, 298−302.
(6) Halliwell, B. *J. Neurochem.* **2006**, *97*, 1634−1658.
(7) Hung, Y.; Bush, A.; Cherny, R. *J. Biol. Inorg. Chem.* **2010**, *15*, 61−76.
(8) Faller, P. *Free Radic. Biol. Med.* **2012**, *52*, 747−748.
(9) Duce, A. I., J. A; Bush. *Prog. Neurobiol.* **2010**, *92*, 1−18.
(10) Dong, J.; Atwood, C. S.; Anderson, V. E.; Siedlak, S. L.; Smith, M. A.; Perry, G.; R., C. P. *Biochemistry* **2003**, *42*, 2768−2773.
(11) Hureau, C.; Faller, P. *Biochimie* **2009**, *91*, 1212−1217.
(12) Karr, J. W.; Kaupp, L. J.; Szalai, V. A. *J. Am. Chem. Soc.* **2004**, *126*, 13534−13538.
(13) Hureau, C. *Coord. Chem. Rev.* **2012**, *256*, 2164−2174.
(14) Shearer, J.; Szalai, V. A. *J. Am. Chem. Soc.* **2008**, *130*, 17826−17835.
(15) Hureau, C.; Balland, V.; Coppel, Y.; Solari, P. L.; Fonda, E.; Faller, P. *J. Biol. Inorg. Chem.* **2009**, *14*, 995−1000.
(16) Furlan, S.; Hureau, C.; Faller, P.; La Penna, G. *J. Phys. Chem. B* **2010**, *114*, 15119−15133.
(17) Hureau, C.; Dorlet, P. *Coord. Chem. Rev.* **2012**, *256*, 2175−2187.
(18) Jiang, D.; Men, L.; Wang, J.; Zhang, Y.; Chickenyen, S.; Wang, Y.; Zhou, F. *Biochemistry* **2007**, *46*, 9270−9282.
(19) Brzyska, M.; Trzesniewska, K.; Wieckowska, A.; Szczepankiewicz, A.; D., E. *ChemBioChem* **2009**, *10*, 1045−1055.
(20) Guilloreau, L.; Combalbert, S.; Sournia-Saquet, A.; Mazarguil, H.; Faller, P. *ChemBioChem* **2007**, *8*, 1317−1325.
(21) Balland, V.; Hureau, C.; Savéant, Jean-Michel. *Proc. Natl. Acad. Sci. U. S. A.* **2010**, *107*, 17113−17118.
(22) Sulpizi, M.; Raugei, S.; VandeVondele, J.; Carloni, P.; Sprik, M. *J. Phys. Chem. B* **2007**, *111*, 3969−3976.
(23) Humphrey, W.; Dalke, A.; Schulten, K. *J. Mol. Graph.* **1996**, *14*, 33−38, http://www.ks.uiuc.edu/Research/vmd.
(24) Dorlet, P.; Gambarelli, S.; Faller, P.; Hureau, C. *Angew. Chem., Int. Ed.* **2009**, *48*, 9273−9276.
(25) Hureau, C.; Coppel, Y.; Dorlet, P.; Solari, P. L.; Sayen, S.; Guillon, E.; Sabater, L.; Faller, P. *Angew. Chem., Int. Ed.* **2009**, *48*, 9522−9525.
(26) Kowalik-Jankowska, T.; M., R.; Wiśniewska, K.; Łankiewicz, L.; Dyba, M. *J. Inorg. Biochem.* **2004**, *98*, 940−950.
(27) Drew, S. C.; Barnham, K. J. *Acc. Chem. Res.* **2011**, *44*, 1146−1155.
(28) Furlan, S.; La Penna, G. *Phys. Chem. Chem. Phys.* **2009**, *11*, 6468−6481.
(29) Kumar, S.; Nussinov, R. *ChemBioChem* **2002**, *3*, 604−617.

(30) Furlan, S.; La Penna, G.; Guerrieri, F.; Morante, S.; Rossi, G. *J. Biol. Inorg. Chem.* **2007**, *12*, 571−583.
(31) Lee, J. Y.; Friedman, J. E.; Angel, I.; Kozak, A.; Y., K. J. *Neurobiol. Aging* **2004**, *25*, 1315−1321.
(32) Adlard, P. A.; et al. *Neuron* **2008**, *59*, 43−55.
(33) Deraeve, C.; Boldron, C.; Maraval, A.; Mazarguil, H.; Gornitzka, H.; Vendier, L.; Pitié, M.; Meunier, B. *Chemistry* **2008**, *14*, 682−696.
(34) Barnham, K. J.; et al. *Proc. Natl. Acad. Sci. U. S. A.* **2008**, *105*, 6813−6818.
(35) Sasaki, I.; Bijani, C.; Ladeira, S.; Bourdon, V.; Faller, P.; Hureau, C. *Dalton Trans.* **2012**, *41*, 6404−6407.